Ultrafast excitonic and charge transfer dynamics in nanostructured organic polymer materials

Matthias Polkehn[a], Pierre Eisenbrandt[a], Hiroyuki Tamura[b], Stefan Haacke[c], Stéphane Méry[c], and Irene Burghardt[a]

[a]Institute of Physical and Theoretical Chemistry, Goethe University Frankfurt, Max-von-Laue-Str. 7, 60438 Frankfurt, Germany
[b]WPI-Advanced Institute for Material Research,Tohoku University, 2-1-1 Katahira, Aoba-ku, Sendai 980-8577, Japan
[c]Institut de Physique et Chimie des Matériaux de Strasbourg, Université de Strasbourg - CNRS, 67034 Strasbourg Cedex 2, France

ABSTRACT

We present theoretical studies of elementary exciton and charge transfer processes in functional organic materials, in view of understanding the key microscopic factors that lead to efficient charge generation in photovoltaics applications. As highlighted by recent experiments, these processes can be guided by quantum coherence, despite the presence of static and dynamic disorder. Our approach combines first-principles parametrized Hamiltonians, based on Time-Dependent Density Functional Theory (TDDFT) and/or high-level electronic structure calculations, with accurate quantum dynamics simulations using the Multi-Configuration Time-Dependent Hartree (MCTDH) method. This contribution specifically addresses charge generation in a novel class of highly ordered oligothiophene-perylene diimide type co-oligomer assemblies, highlighting that chemical design of donor/acceptor combinations needs to be combined with a detailed understanding of the effects of molecular packing.

Keywords: Organic photovoltaics, exciton dissociation, charge transfer, quantum dynamics

1. INTRODUCTION

Besides the chemical composition of the relevant donor-acceptor (DA) materials, efficient charge separation in organic photovoltaics depends to a large extent on the materials' morphology. For example, bulk heterojunctions (BHJ)[1,2] allow for efficient exciton diffusion to the DA interface, and are compatible with nanoscale ordering that possibly enhances exciton and carrier mobilities. Here, we focus upon alternative architectures that rely on the self-assembly of covalently bound DA block co-polymers or co-oligomers.[3–6] We specifically address recently developed oligothiophene-perylene diimide (OT-PDI) based DA dyad and DAD triad combinations that are organized in smectic liquid crystalline (LC) films[7] or else lamellar mesophases.[8,9]

Spectroscopic investigations of two generations of the abovementioned DA(D) systems have shown widely different types of kinetics, ranging from ultrafast (subpicosecond) generation of charges that are subject to rapid recombination[7,10] to much slower (tens of picoseconds) charge generation yielding long-lived CT states.[11] These two generations of materials with the same basic constituents differ both in the details of chemical design and in their nanoscale architecture. Hence, several factors could contribute to the observed kinetics.

Against this background, a combination of electronic structure investigations, first-principles parametrized model Hamiltonians, and high-dimensional quantum dynamics is employed to provide insight both into the effect of chemical design and molecular packing upon charge generation in the above donor-acceptor materials. The present study summarizes our findings on the electronic structure properties of the two generations of materials, highlights the importance of intermolecular interactions in the first-generation material, and provides evidence for coherent quantum effects on ultrafast time scales.

---

2. FIRST AND SECOND GENERATION BISTHIOPHENE-PERYLENE SYSTEMS

In this section, we address two generations of oligothiophene-perylene diimide based co-oligomers that are organized in smectic liquid crystalline (LC) films[7, 12] or else lamellar mesophases.[8, 9] These systems have been investigated by time-resolved optical spectroscopy, both in solution and in LC phase.[7, 10] The discussion of this section focuses upon the electronic properties of these DA combinations.

2.1 First-generation DAD triads

Co-oligomers of bisthiophene-PDI type were first designed as DAD triads,[7, 10, 12] as illustrated in Figure 1. These triad species exhibit a remarkably different photochemistry in chloroform solution[10] and smectic LC films,[7] as summarized in the figure. In solution, the DAD system exhibits ultrafast ($\sim$130 fs) excitation energy transfer (EET) from the donor to the acceptor moiety, followed by slower (2.7 ps) charge separation.[10] By contrast, the dynamics in a smectic LC film shows ultrafast ($\sim$60 fs) charge transfer in the absence of EET.[7] Despite the efficient CT formation in the LC phase, recombination within $\sim$50 ps as well as triplet formation on a longer time scale ($>$ 1 ns) were found to severely limit the transient photocurrent.
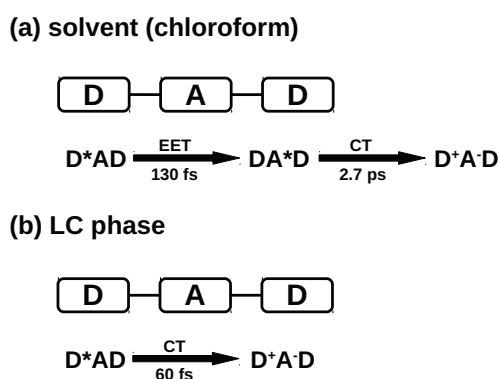
Figure 1. Schematic illustration of the kinetic pathways of the first-generation DAD triad system in solution and LC phase. The time scales for the EET and CT steps have been obtained from pump-probe spectroscopy.[7, 10]

As detailed in Ref. [13] and illustrated in Figure 2, the electronic transitions in the DAD system can be understood in terms of well-separated excitations of the D and A moieties (denoted D-XT and A-XT in the figure), along with a principal intramolecular charge transfer (CT) state. To reduce the computational effort, electronic structure calculations were carried out for DA dyad species rather than DAD triads, given that the relevant electronic properties are expected to be essentially unchanged.[13, 14]
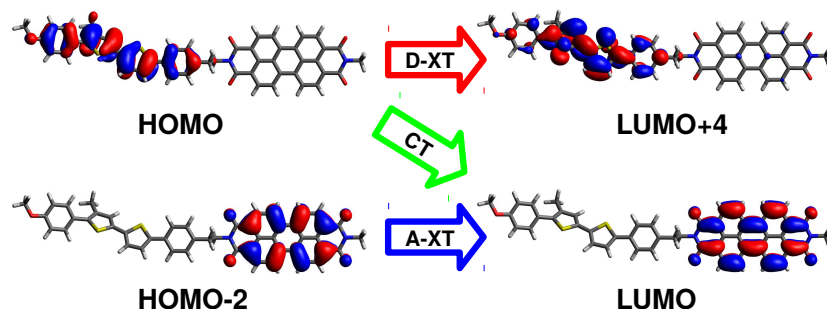
Figure 2. Principal electronic transitions in the DA system, including local excitations of the donor moiety (D-XT) and acceptor moiety (A-XT), along with a D$\rightarrow$A charge transfer transition. Calculations were carried out at the TDDFT level, with suitable benchmarks using the Second-Order Approximate Coupled-Cluster (CC2) approach.

2.2 Second-generation D_nA dyads

In view of the inefficient charge generation in the first-generation DAD system, a second generation of D_nA dyad co-oligomers was devised[8,9] with the aim of increasing the CT lifetime while preserving a near 100% CT formation efficiency. An increased CT lifetime is indicative of a reduced recombination rate and a higher photocurrent yield. This new co-oligomer generation features both chemical modifications and a different molecular packing as compared with the first-generation material. As detailed in Refs. [8,9], the second-generation material is organized into highly ordered lamellar mesophases that feature well-defined donor and acceptor domains; the latter are interleaved such as to form a zipper-like structure.[9]

As for the aspect of chemical design, the donor and acceptor cores are closely related to the first-generation material, but additional linking moieties are now sandwiched between the D and A parts, as illustrated in Figure 2. Notably, the additional δ (benzene containing) and δ^+ (benzothiadiazol containing) variants are investigated. In addition, a δ^- (amino) moiety is optionally attached to the donor building blocks (not shown in Figure 3). Finally, several D units may be concatenated to form, e.g., $\delta^- D_n \delta^+ A$ units, whose length tends to increase both the CT formation time and the CT lifetime.[11]
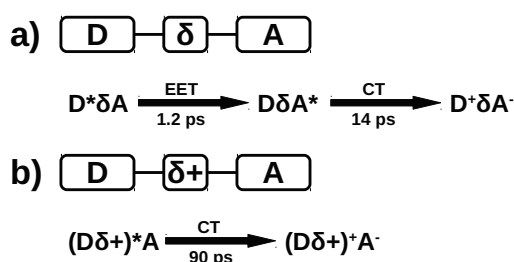
Figure 3. Schematic illustration of $D\delta A$ and $D\delta^+ A$ species and the relevant EET and CT transfer steps from time-resolved spectroscopy.[11] The measured time scales refer to solution phase measurements with chloroform solvent.

Spectroscopic investigation reveals that in the presence of the δ spacer, the transfer mechanism remains similar to the first-generation material (see Figure 3a), such that donor-acceptor excitation energy transfer precedes charge transfer. The main effect of the spacer is an increase of both EET and CT time scales. However, in the presence of the δ^+ spacer, the mechanism changes distinctly (see Figure 3b): the EET step is now absent, and charge transfer occurs directly from the photoexcited donor $(D\delta^+)$ moiety, on a time scale of $\sim$90 ps. Further, the δ^- (amino) moiety leads to a significant (up to threefold) extension of the CT lifetime.
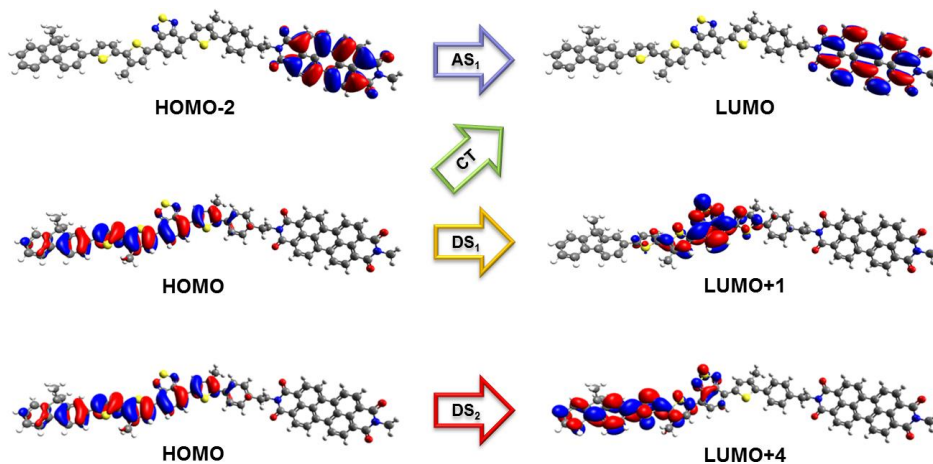
Figure 4. Excited-state electronic structure of $D\delta^+ A$ species, showing the most relevant electronic transitions. As compared with Figure 1, note the additional excitation on the δ^+ moiety (DS_1) which is now involved in the D-A charge transfer.

The spectroscopic observations are corroborated by electronic structure analysis (see Figure 4), revealing an additional excitation on the δ^+ moiety (DS$_1$) in addition to the principal donor transition (DS$_2$). A more detailed analysis[11] confirms that this transition is involved in the (Dδ^+)→A charge transfer.

3. CHARGE SEPARATION IN LIQUID CRYSTALLINE PHASE

As shown above, charge transfer time scales and CT state lifetimes in solution are comparatively long, ranging from few to tens of picoseconds. This is in striking contrast to the ultrafast charge transfer observed in the first-generation liquid-crystalline DAD systems[7] (see Figure 1b), suggesting the possibility that an additional pathway could arise from the specific molecular packing of the LC phase. We have therefore undertaken a combined electronic structure and quantum dynamical analysis[14] that is tailored to the nanoscale order of the LC phase.

Figure 5 illustrates the model structure under study, taken from the X-ray structure of the liquid crystalline material.[12] A prominent feature of the smectic LC phase is the large tilt angle of ∼70° between the molecular plane and the normal plane of the crystal. As a consequence, an initially delocalized exciton extended across several donor moieties is of J-aggregate[15, 16] type (rather than of H-aggregate[15, 16] type as one would expect for a vertically stacked DA array). As a second consequence, intermolecular π-stacking does not occur between the same types of monomers (D or A), but rather between D-A neighbors belonging to adjacent DAD segments, as illustrated in Figure 5. Hence, one might expect that intermolecular DA interactions could effectively compete with intramolecular EET and CT processes.
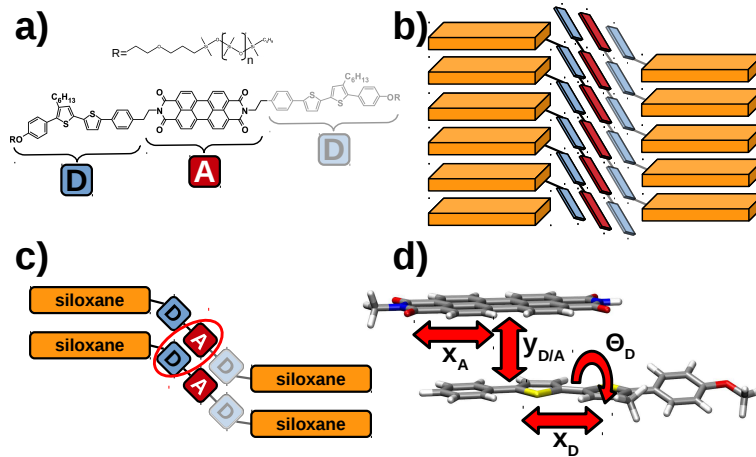
Figure 5. (a) Molecular structure of the isolated DAD system, where R represents siloxane side chains. (b) Schematic representation of the smectic LC phase stabilized by the stacking of the siloxane side chains. (c) Fragment taken from the supramolecular assembly in the smectic LC phase. (d) Molecular structure of a stacked D-A pair corresponding to the LC phase geometry, with the most relevant nuclear modes. Reproduced with permission from Ref. 14.

To elucidate the elementary processes in the LC phase, we combine electronic structure calculations for selected fragments with a vibronic Hamiltonian in a generalized electron-hole (e-h) representation,[17, 18] $|\nu_e \mu_h\rangle \equiv |\nu\mu\rangle$, where the electron is located at site $\nu_e = \nu$ while the hole is located at site $\mu_h = \mu$. Localized e-h pairs $|\nu\nu\rangle$ correspond to Frenkel excitonic (XT) configurations on the D or A moieties, $|D_i^{XT}\rangle = |\nu = i, \mu = i\rangle$ (where $i = 1, \ldots, N_D$) and $|A_j^{XT}\rangle = |\nu = j, \mu = j\rangle$ (where $j = 1, \ldots, N_A$). Conversely, non-local e-h states $|\nu\mu\rangle$, $\mu \neq \nu$ ($\nu = 0$, $\mu = 1$, ..., N), represent charge-separated (CS) configurations, $|D_i^+ A_j^-\rangle = |\nu_i \mu_j\rangle$. We also use the short-hand notation CS(n) to denote the subset of CS configurations with an electron-hole separation of $i - j \equiv n$.

In the e-h basis specified above, the Hamiltonian takes the following form,

$$\hat{H} = \hat{H}_{\text{on-site}} + \hat{H}_{\text{coupl}} + \hat{H}_{\text{e-ph}} \tag{1}$$
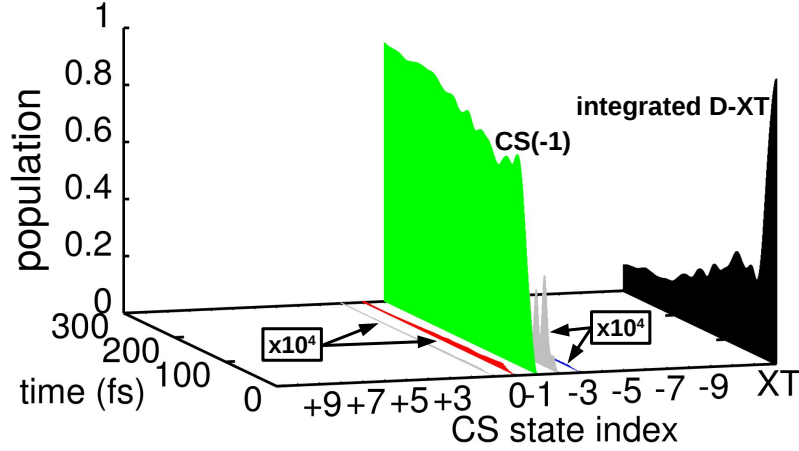
Figure 6. Full quantum dynamical evolution for the coupled excitonic donor and CS manifolds (156 states, 48 modes) obtained from Multi-Layer Multi-Configuration Time-Dependent Hartree (ML-MCTDH) calculations.[14] The ultrafast decay ($\sim$50 fs) of the excitonic donor states is matched by a rise in the CS(-1) manifold while other CS(n) states are barely populated due to the comparatively high Coulomb barrier and small transfer integrals. Reproduced with permission from Ref. 14.

where $\hat{H}_{\text{el}}$ refers to the electronic Hamiltonian including on-site energies ($\hat{H}_{\text{on-site}}$) and intra- and inter-molecular electronic couplings ($\hat{H}_{\text{coupl}}$), while $\hat{H}_{\text{e-ph}}$ represents the phonon (vibrational) Hamiltonian including electron-phonon (e-ph) coupling. The explicit form of these contributions is given in the following. First, for the on-site energies,

$$\hat{H}_{\text{on-site}} = \epsilon_D \sum_{i=1}^{N_D} |D_i^{XT}\rangle\langle D_i^{XT}| + \epsilon_A \sum_{i=1}^{N_A} |A_i^{XT}\rangle\langle A_i^{XT}| + \sum_{i=1}^{N_D}\sum_{j=1}^{N_A} \epsilon_{D_i^+ A_j^-} |D_i^+ A_j^-\rangle\langle D_i^+ A_j^-| \tag{2}$$

where the on-site energies of the excitonic donor (ϵ_D) or acceptor (ϵ_A) states are taken to be equal for all fragments, while the energies of the CS states ($\epsilon_{D_i^+ A_j^-}$) are defined by an effective Coulomb barrier.[14] The on-site energies ϵ_D, ϵ_A, and $\epsilon_{D_i^+ A_j^-}$ for Frenkel states and nearest-neighbor electron-hole states (i.e., e-h distance $|i-j| \leq 1$) have been determined by Algebraic Diagrammatic Construction Scheme (ADC(2)) calculations for a stacked DA dimer fragment at the Franck-Condon geometry as shown in Figure 5d, while the on-site energies for charge-separated states with large electron-hole distances $|i-j| > 1$ rely on complementary TDDFT calculations for larger fragments that were used to determine the Coulomb barrier.

Next, the electronic coupling part of the Hamiltonian reads as follows,

$$\begin{aligned}
\hat{H}_{\text{coupl}} &= J_D \sum_{i=1}^{N_D}\sum_{j=1}^{N_D} (|D_i^{XT}\rangle\langle D_j^{XT}| + \text{h.c.}) + J_A \sum_{i=1}^{N_A}\sum_{j=1}^{N_A} (|A_i^{XT}\rangle\langle A_j^{XT}| + \text{h.c.}) \\
&+ J_{DA} \sum_{i=1}^{N_D}\sum_{j=1}^{N_A} (|D_i^{XT}\rangle\langle A_j^{XT}| + \text{h.c.}) \\
&+ \kappa_D \sum_{i=1}^{N_D}\sum_{j=1}^{N_A} (|D_i^{XT}\rangle\langle D_i^+ A_j^-| + \text{h.c.}) + \kappa_A \sum_{i=1}^{N_A}\sum_{j=1}^{N_A} (|A_i^{XT}\rangle\langle D_j^+ A_i^-| + \text{h.c.}) \\
&+ t_e \sum_{i=1}^{N_D}\sum_{j=2}^{N_A-1} (|D_i^+ A_j^-\rangle\langle D_i^+ A_{j\pm1}^-| + \text{h.c.}) + t_h \sum_{i=2}^{N_D-1}\sum_{j=1}^{N_A} (|D_i^+ A_j^-\rangle\langle D_{i\pm1}^+ A_j^-| + \text{h.c.})
\end{aligned} \tag{3}$$

describing various types of intra- and intermolecular couplings, i.e., excitonic couplings between donor and acceptor species (J_D, J_A, J_{AD}), charge transfer from excitonic states to intramolecular CT states or charge-

separated stacked donor/acceptor pairs (κ_D, κ_A), and transfer integrals for electron and hole transfer (t_e, t_h) that determine the transient conductivity of the separated carriers. The pairwise (ij) interactions are restricted to nearest-neighbor couplings in our current analysis.

Finally, the Hamiltonian is going to be modulated by vibronic (e-ph) couplings $\hat{H}_{\text{e-ph}}$ according to Eq. (1), which are included in terms of state-dependent potential energy surfaces (PES) as detailed in Ref. [14].

The efficiency of the various competing transfer pathways depends on the magnitude of the respective couplings and on the resonance offsets determined by $\hat{H}_{\text{on-site}}$. Our analysis[14] shows that (i) the excitonic coupling is sizeable ($J_D = -0.1$ eV) and will lead to initial delocalization at the lower band edge of the donor J-aggregate, (ii) the intra-chain charge transfer coupling ($\kappa_D^{\text{intra}} = 0.002$ eV) is much weaker than the intermolecular charge transfer coupling ($\kappa_D^{\text{inter}} = 0.025$ eV), (iii) the transfer integrals for electron ($t_e = 0.0005$ eV) and hole ($t_e = 0.0013$ eV) transport are small.

The results of our quantum dynamical simulations are summarized in Figure 6, showing a rapid decay of the excitonic donor population and concomitant rise of the CS state population, on an initial time scale of $\sim$50 fs. Cumulative populations are shown, i.e., $P_D^{XT} = \sum_i P_{D_i}^{XT}$ and $P_{\text{CS}(n)} = \sum_{i,j} P_{D_i^+ A_j^-}$ (for $i - j = n$). Strikingly, practically all population accumulates in the CS($n = -1$) states. This is due to (i) the unfavorable energetics of the CS($n \neq -1$) states resulting from the Coulomb barrier, and (ii) the small transfer integrals (t_e, t_h), precluding a rapid formation of photocurrent. After $\sim$250 fs, the charge transfer is essentially complete and a quasi-stationary state of the CS(-1) populations is reached.

The above time scales are in excellent agreement with the CT formation time deduced from experiment for the LC film (i.e., $\sim$60 fs),[7] along with the observation that recombination rather than photocurrent formation apparently dominates in the first-generation LC material.

4. CONCLUSION

The present study underscores that new transfer channels may open up, depending on the material's nano-morphology. In the case of the first-generation material addressed above, intermolecular charge transfer dominates in the particular LC architecture under study, resulting in ultrafast CT time scales. By contrast, a much slower intramolecular CT process is observed in the second-generation materials. Interestingly, a very similar situation was observed for slip-stacked donor-acceptor assemblies composed of oligo(p-phenylene vinylene) (OPV) and perylene diimide units.[19] In this system, intermolecular charge transfer was again found to be by far dominant, in contrast to an H-aggregate assembly of the same donor-acceptor units, where slower intramolecular charge transfer prevails.[19]

Hence, chemical design at the level of the isolated DA species needs to be complemented by the study of both dielectric effects and the influence of molecular packing. The combined effects of intramolecular and intermolecular excitonic and charge transfer interactions may lead to intriguing photophysical and transport properties that necessitate a detailed spectroscopic and theoretical analysis. In this context, the present first-principles theoretical framework offers a consistent approach that can be adapted to related aggregation patterns and donor-acceptor materials.

REFERENCES

[1] Deibel, C., Strobel, T., and Dyakonov, V., "Role of the Charge Transfer State in Organic Donor-Acceptor Solar Cells," *Adv. Mater.* **22**, 4097–4111 (2010).

[2] Hwang, I. W., Soci, C., Moses, D., Zhu, Z., Waller, D., Gaudiana, R., Brabec, C. J., and Heeger, A., "Ultrafast Electron Transfer and Decay Dynamics in a Small Band Gap Bulk Heterojunction Material," *Adv. Mater.* **19**, 2307–2312 (2007).

[3] Bu, L., Guo, X., Yu, B., Qu, Y., Xie, Z., Yan, D., Geng, Y., and Wang, F., "Monodisperse Co-oligomer Approach toward Nanostructured Films with Alternating Donor-Acceptor Lamellae," *J. Am. Chem. Soc.* **131**, 13242–13243 (2009).

[4] Gao, B., Qu, J., Wang, Y., Fu, Y., Wang, L., Chen, Q., Sun, H., Geng, Y., Wang, H., and Xie, Z., "Femtosecond Spectroscopic Study of Photoinduced Charge Separation and Recombination in the Donor-Acceptor Co-Oligomers for Solar Cells," *J. Phys. Chem. C* **117**, 4836–4843 (2013).

[5] Guo, C., Lin, Y., Witman, M. D., Smith, K. A., Wang, C., Hexemer, A., Strzalka, J., Gomez, E. D., and Verduzco, R., "Conjugated Block Copolymer Photovoltaics with near 3% Efficiency Through Microphase Separation," *NANO Letters* **13**, 2957–2963 (2013).

[6] Lee, Y. and Gomez, E. D., "Challenges and Opportunities in the Development of Conjugated Block Copolymers for Photovoltaics," *Macromolecules* **48**, 7385–7395 (2015).

[7] Roland, T., Léonard, J., Hernandez Ramirez, G., Méry, S., Yurchenko, O., Ludwigs, S., and Haacke, S., "Sub-100 fs Charge Transfer in a Novel Donor-Acceptor-Donor Triad Organized in a Smectic Film," *Phys. Chem. Chem. Phys.* **14**, 273–279 (2012).

[8] Schwartz, P.-O., Biniek, L., Zaborova, E., Heinrich, B., Brinkmann, M., Leclerc, N., and Méry, S., "Perylenediimide-Based Donor-Acceptor Dyads and Triads: Impact of Molecular Architecture on Self-Assembling Properties," *J. Am. Chem. Soc.* **136**, 5981–5992 (2014).

[9] Biniek, L., Schwartz, P.-O., Zaborova, E., Heinrich, B., Leclerc, N., Méry, S., and Brinkmann, M., "Zipper-Like Molecular Packing of Donor-Acceptor Conjugated Co-Oligomers Based on Perylenediimide," *J. Mater. Chem. C* **3**, 3342–3349 (2015).

[10] Roland, T., Hernandez Ramirez, G., Léonard, J., Méry, S., and Haacke, S., "Ultrafast Broadband Laser Spectroscopy Reveals Energy and Charge Transfer in Novel Donor-Acceptor Triads for Photovoltaic Applications," *J. Phys.: Conf. Ser.* **276**, 012006 (2011).

[11] Liu, L., Eisenbrandt, P., Roland, T., Polkehn, M., Schwartz, P.-O., Bruchlos, K., Omiecienski, B., Ludwigs, S., Leclerc, N., Zaborova, E., Léonard, J., Méry, S., Burghardt, I., and Haacke, S. (2016). Controlling Charge Separation and Recombination by Chemical Design in Donor-Acceptor Dyads, submitted to Phys. Chem. Chem. Phys. (2016).

[12] Ramirez, G. H. (2010). Ph.D. Thesis, Université de Strasbourg, http://tel.archives-ouvertes.fr/tel-00579777/fr/.

[13] Wenzel, J., Dreuw, A., and Burghardt, I., "Charge and Energy Transfer in a Bithiophene Perylenediimide Based Donor-Acceptor-Donor System for Use in Organic Photovoltaics," *Phys. Chem. Chem. Phys.* **15**, 11704–11716 (2013).

[14] Polkehn, M., Tamura, H., Eisenbrandt, P., Haacke, S., Méry, S., and Burghardt, I. (2016). Molecular Packing Determines Charge Separation in a Liquid Crystalline Bisthiophene-Perylene Diimide Donor-Acceptor Material, *J. Phys. Chem. Lett.*, doi:10.1021/acs.jpclett.6b00277.

[15] May, V. and Kühn, O., [*Charge and Energy Transfer Dynamics in Molecular Systems*], 3rd ed., VCH-Wiley (2011).

[16] Spano, F. C. and Silva, C., "H- and J-Aggregate Behavior in Polymeric Semiconductors," *Annu. Rev. Phys. Chem.* **65**, 477–500 (2014).

[17] Merrifield, R. E., "Ionized States in a One-Dimensional Molecular Crystal," *J. Chem. Phys.* **34**, 1835–1839 (1961).

[18] Binder, R., Wahl, J., Römer, S., and Burghardt, I., "Coherent Exciton Transport Driven by Torsional Dynamics: A Quantum Dynamical Study of Phenylene-Vinylene Type Conjugated Systems," *Faraday Discuss.* **163**, 205–222 (2013).

[19] Beckers, E., Meskers, S., Schenning, A., Chen, Z., Würthner, F., Marsal, P., Beljonne, D., Cornil, J., and Janssen, R., "Influence of Intermolecular Orientation on the Photoinduced Charge Transfer Kinetics in Self-Assembled Aggregates of Donor-Acceptor Arrays," *J. Am. Chem. Soc.* **128**, 649–657 (2006).